

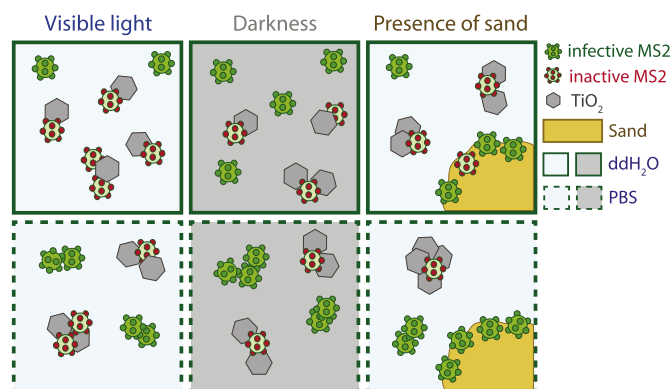
# Inactivation of MS2 bacteriophage by titanium dioxide nanoparticles in the presence of quartz sand with and without ambient light



Vasiliki I. Syngouna\*, Constantinos V. Chrysikopoulos

School of Environmental Engineering, Technical University of Crete, 73100 Chania, Greece

## GRAPHICAL ABSTRACT



## ARTICLE INFO

### Article history:

Received 18 January 2017

Revised 24 February 2017

Accepted 24 February 2017

Available online 27 February 2017

### Keywords:

TiO<sub>2</sub>  
MS2  
Inactivation  
Ambient light  
Darkness  
Quartz sand

## ABSTRACT

Virus inactivation by nanoparticles (NPs) is hypothesized to affect virus fate and transport in the subsurface. This study examines the interactions of viruses with titanium dioxide (TiO<sub>2</sub>) anatase NPs, which is a good disinfectant with unique physicochemical properties. The bacteriophage MS2 was used as a model virus. A series of batch experiments of MS2 inactivation by TiO<sub>2</sub> NPs were conducted at room temperature (25 °C), in the presence and absence of quartz sand, with and without ambient light. Three sets of experiments were performed in phosphate buffered saline solution (PBS) and one in distilled deionized water (ddH<sub>2</sub>O). The virus inactivation experimental data were satisfactorily fitted with a pseudo-first order expression with a time dependent rate coefficient. Quartz sand was shown to affect MS2 inactivation by TiO<sub>2</sub> NPs both in the presence and absence of ambient light, because, under the experimental conditions of this study, the quartz sand offers a protection to the attached MS2 against inactivation. Moreover, it was shown that low TiO<sub>2</sub> concentration (10 mg/L) affected only slightly MS2 inactivation with and without ambient light. Furthermore, PBS hindered MS2 inactivation by TiO<sub>2</sub> NPs.

© 2017 Elsevier Inc. All rights reserved.

## 1. Introduction

Pathogenic viruses present in groundwater are likely to originate from various fecal sources [1,2]. Also, the fate and transport

of pathogenic viruses in groundwater is controlled mainly by attachment onto the solid matrix, and inactivation or loss of infective capability [3–11].

Titanium dioxide (titania, TiO<sub>2</sub>) nanoparticles (NPs) are employed in various consumer products and applications, and easily can be introduced to the aquatic environment [12–15]. TiO<sub>2</sub> exists as three different polymorphs: anatase, rutile, and bro-

\* Corresponding author.

E-mail address: [vsyngouna@isc.tuc.gr](mailto:vsyngouna@isc.tuc.gr) (V.I. Syngouna).

kite [16]. Moreover, the efficient photo-reactivity exhibited by nano-sized TiO<sub>2</sub> makes it an excellent catalyst for wastewater treatment [17]. TiO<sub>2</sub> NPs can enter the aquatic environment either directly or indirectly from various sources, including: sunscreen lotions, nano-paints, food additives, groundwater remediation, and wastewater treatment plant effluents [18–20]. When NPs eventually enter water supplies, their possible interactions with aquatic organisms is an important concern.

The antibacterial properties of TiO<sub>2</sub> have been well documented in the literature [21–24]. Also, TiO<sub>2</sub> NPs are instrumental to the generation of chemically reactive oxygen species (ROS), especially hydroxyl free radicals (HO<sup>•</sup>) and hydrogen peroxide (H<sub>2</sub>O<sub>2</sub>) [25]. While fewer studies have investigated the antiviral properties of TiO<sub>2</sub>, its potential to inactivate viruses has been demonstrated by various investigators [21,22,26–28]. Moreover, water disinfection studies have shown that suspended TiO<sub>2</sub> is more active than TiO<sub>2</sub> immobilised onto surfaces [29,30]. This is attributed to the increased contact between the TiO<sub>2</sub> particles and suspended microorganisms [31].

Several studies have shown that metal ions and TiO<sub>2</sub> NPs photocatalytic reactions under UV radiation provide high rates of disinfection [32–37]. Moreover, other studies examined the photocatalytic property of TiO<sub>2</sub> NPs under visible light illumination [38], whereas a handful of studies focussed on the toxicity of TiO<sub>2</sub> NPs under ambient light conditions [24,39–41]. However, it is not fully understood how ambient light and darkness, which have little or no antimicrobial and antiviral activities, affect microorganism, and more specifically virus inactivation by TiO<sub>2</sub> NPs. Most of the previous studies examined the photocatalytic bacteria and virus inactivation using high concentrations of titanium dioxide. To our knowledge, virus inactivation by TiO<sub>2</sub> NPs at low exposure concentrations (10 mg/L), which can be found in aquatic environments, has not been investigated yet.

The aim of this study was to elucidate the ability of TiO<sub>2</sub> NPs to inactivate MS2 viruses, in both the presence and absence of ambient light, representing surface and subsurface conditions, respectively. Moreover, it was investigated whether MS2 inactivation by TiO<sub>2</sub> NPs can be enhanced in the presence of quartz sand under both ambient light and dark conditions. For these experiments, three different virus concentrations were tested. Furthermore, a comparison between MS2 inactivation in ddH<sub>2</sub>O and PBS in the presence and absence of quartz sand with and without ambient light was performed. Also, possible mechanistic interpretations of synergistic effects were discussed.

## 2. Materials and methods

### 2.1. Preparation of virus suspension

The bacteriophage MS2 (ATCC 15597-B1) with host bacterium the *E. coli* (ATCC 15597) was used as a model virus in this study, due to its similarity to many waterborne pathogenic viruses and to its propagation and enumeration simplicity. MS2 samples were enumerated according to the double agar layer method [42]. Briefly, 100 μL of the host bacterium *E. coli* (ATCC 15597-B1) and 100 μL of a diluted MS2 virus sample were mixed in a centrifuge tube with 4.5 mL of molten soft-agar medium maintained at 45 °C. Then, the mixture was poured onto a petri dish containing solid Tryptic Soy Agar (TSA) medium. After overnight incubation at 37 °C, infective MS2 concentrations were determined by counting the number of plaques in *E. coli* lawn, and reported as plaque-forming units per milliliter (PFU/mL). All samples were analyzed either immediately or after 24-h storage at 4 °C in the dark. No change in viral titers was observed over a 24-h storage, neither in the presence nor the absence of the TiO<sub>2</sub> NPs.

### 2.2. Preparation of TiO<sub>2</sub> NPs suspensions and quartz sand

TiO<sub>2</sub> NPs (anatase), 99.9% pure, with a primary particle size less than 25 nm (Sigma-Aldrich Corporation) were used in all experiments. A stock suspension of TiO<sub>2</sub> NPs (1 g/L) was prepared by adding TiO<sub>2</sub> NP powder into distilled deionized water (ddH<sub>2</sub>O), followed by a 30 min ultrasonication (Elma Transonic TI-H-5 ultrasonicator). TiO<sub>2</sub> NP suspensions (10 mg/L) were prepared by diluting the stock suspension into prepared solutions of phosphate buffered saline solution (PBS) at pH = 7 and ionic strength (I<sub>s</sub>) of 2 mM. The zeta potential of TiO<sub>2</sub> NPs in both ddH<sub>2</sub>O and PBS (pH = 7) by a zetasizer (Nano ZS90, Malvern Instruments, Southborough, MA), and was determined to be  $-23.7 \pm 0.9$  mV and  $-30.1 \pm 1.0$  mV, respectively.

Quartz sand (Filcom Filterzand & Grind) with a size range of 0.425–0.600 mm, and approximate average diameter of 0.513 mm were used in this study. Prior to each experiment, the sand was cleaned with 0.1 M HNO<sub>3</sub> (70%) for a 3-h time period to remove surface impurities (e.g., iron hydroxide and organic coatings) that could promote physicochemical deposition of the viruses, rinsed with ddH<sub>2</sub>O, then soaked in 0.1 M NaOH for a 3-h time period, and rinsed again with ddH<sub>2</sub>O. Subsequently, the sand was dried in an oven at 105 °C, and then stored in screw cap sterile beakers until use in the batch experiments. The zeta potential of the quartz sand in PBS solution under the experimental conditions (pH = 7, I<sub>s</sub> = 2 mM) was measured equal to  $-62.3 \pm 3.5$  mV [8].

### 2.3. Characterization of untreated TiO<sub>2</sub> NPs

To characterize the crystalline size and structure of untreated (“as shipped”) TiO<sub>2</sub> NPs, powdered X-ray diffraction analysis (XRD) was carried out (Bruker D8 advance diffractometer with Ni-filtered Cu K $\alpha$  radiation and a LynxEye detector). The XRD pattern was obtained at a 2 $\theta$  range from 2° to 70°, scanned at a scanning angle increment of 0.015° with a time step of 0.3 s (see Fig. 1). Furthermore, the particle size of the untreated TiO<sub>2</sub> NPs was analysed using Transmission Electron Microscopy (TEM) (JEOLJEM-2100 system, operated at 200 kV). TiO<sub>2</sub> NP suspensions (10 mg/L), in both ddH<sub>2</sub>O and PBS, were placed in an ultrasonic bath for 30 min, air-dried onto a carbon-coated copper grid (200 mesh) and subjected to TEM analysis. Two representative TEM images are shown in Fig. 2. The TEM images suggested that suspended TiO<sub>2</sub> NPs were significantly aggregated in both ddH<sub>2</sub>O and PBS, in concordance with previous publications [43–46]. Also, the TEM images showed that the suspended TiO<sub>2</sub> NPs were essentially spherical.

### 2.4. Stability of TiO<sub>2</sub> NPs

Prior to the initiation of the TiO<sub>2</sub> suspension stability and aggregation experiments, the TiO<sub>2</sub> stock suspension (1 g/L) was soni-

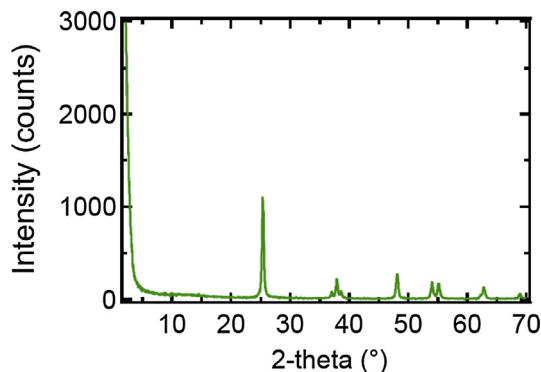
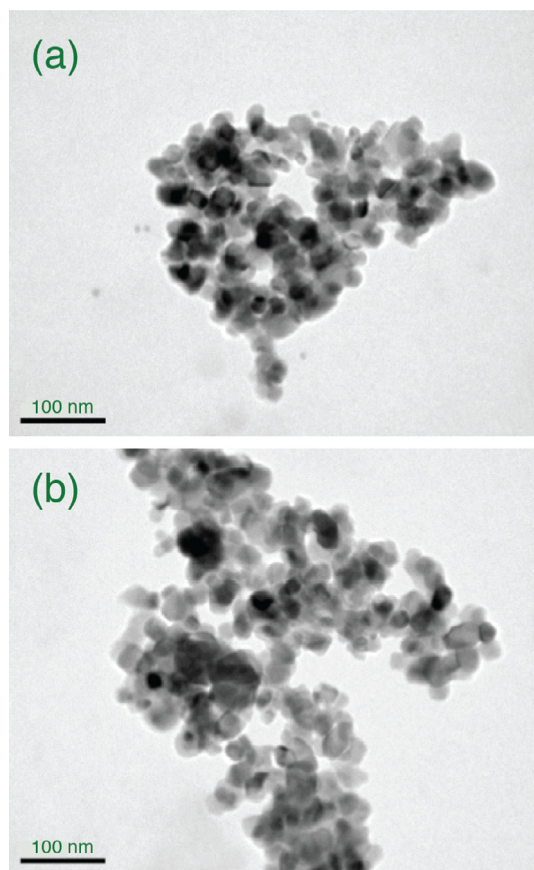


Fig. 1. X-ray diffraction pattern of TiO<sub>2</sub> powder (anatase).



**Fig. 2.** Transmission electron micrographs of TiO<sub>2</sub> (anatase) in: (a) ddH<sub>2</sub>O, and (b) PBS.

cated for 30 min in order to homogenize and monodisperse the samples. Subsequently, 500 mL of the TiO<sub>2</sub> suspension were added to a glass beaker and allowed to settle undisturbed over a 7-d time period. However, a 5-mL aliquot of the supernatant liquid was carefully sampled once a day from the top of the glass beaker (~2 cm below surface). From each sample collected, the corresponding TiO<sub>2</sub> NP concentration and particle size were determined and recorded. The TiO<sub>2</sub> NP concentrations were determined using a UV-visible spectrophotometer at a wavelength 287 nm. The UV-vis absorption spectra of several TiO<sub>2</sub> NPs concentrations in PBS solution, and the corresponding calibration curve can be found in the [supporting information](#) (see Figs. S1 and S2). The average TiO<sub>2</sub> NP aggregate sizes (hydrodynamic diameters) were measured by dynamic light scattering (DLS) (Zetasizer Nano-ZS analyzer, Malvern Instrument Inc., U.K.), and the observed TiO<sub>2</sub> NP size distribution for the 7-d time period tested can be found in the [supporting information](#) (see Fig. S3).

### 2.5. Batch experiments

The batch experiments of MS2 inactivation by TiO<sub>2</sub> NPs both in the absence and the presence of quartz sand were conducted in 50-mL glass “reactor tubes” by diluting MS2 stock solution in 50 mL suspension of TiO<sub>2</sub> NPs in ddH<sub>2</sub>O or PBS solution (10 mg/L), which also contained 5 g of dry clean quartz sand. Three initial virus concentrations,  $C_0$  ( $1.7 \pm 0.22 \times 10^3$ ,  $1 \pm 0.14 \times 10^4$ , and  $8.7 \pm 1.8 \times 10^6$  PFU/mL) were chosen for the experiments in PBS and one ( $2.1 \pm 0.59 \times 10^4$  PFU/mL) for the experiments in ddH<sub>2</sub>O. The batch inactivation experiments were conducted under both ambient light and dark conditions. For the experiments under dark

conditions, the glass tubes were carefully covered by aluminum foil. Batch MS2 inactivation experiments were also conducted in 50-mL glass “control tubes” in the absence of TiO<sub>2</sub> NPs and quartz sand. Note that the control and reactor tubes were treated in the same manner. Moreover, all materials that came in contact with the MS2 solutions were sterilized by autoclaving. Throughout the settling period, a relatively uniform thin layer of sand grains was formed on the bottom of the tubes and 2 mL sub-samples were withdrawn at different time intervals (0, 0.010, 0.021, 0.042, 0.083, 0.121, 1, 2, 3, 4, 5, 7, 15, 20, 30 days) from the top of each reactor or control tube (~2 cm below surface) and the total (suspended + attached onto TiO<sub>2</sub> NPs) concentration of MS2 was assayed by the double-layer overlay method [42], as outlined by Syngouna and Chrysikopoulos [7].

### 3. Theoretical considerations

Previous studies on photocatalytic inactivation of viruses by TiO<sub>2</sub> are often modeled using pseudo-first-order kinetics (e.g., Chick-Watson) [26,47,48], referring to either the liquid-phase (suspended) or the total (suspended + attached) concentration of viruses. Note that the inactivation rates of suspended and attached viruses should not be assumed equal [49,50]. Moreover, virus inactivation rate coefficients are not constant and exhibit temporal variability due to the existence of various virus subpopulations with different inactivation rate coefficients [3]. Thus, numerous virus inactivation studies have employed the following pseudo-first-order expression with a time-dependent inactivation rate coefficient [51–58]:

$$\frac{dC(t)}{dt} = -\lambda(t)C(t) \quad (1)$$

where  $C$  is the concentration of total (suspended and attached onto TiO<sub>2</sub> NPs) viruses in the liquid phase,  $t$  is time, and  $\lambda$  is the time-dependent inactivation rate coefficient of total viruses described by the following expression:

$$\lambda(t) = \lambda_0 e^{-\alpha t} \quad (2)$$

where  $\lambda_0$  is the initial inactivation rate coefficient, and  $\alpha$  is the resistivity coefficient. Assuming that  $C(0) = C_0$ , where  $C_0$  is the initial virus concentration, the solution to Eq. (1) is:

$$\ln \left[ \frac{C(t)}{C_0} \right] = \frac{\lambda_0}{\alpha} \{ \exp[-\alpha t] - 1 \} \quad (3)$$

For the special case where  $\lambda(t) = \lambda$  the solution to Eq. (1) is:

$$\ln \left[ \frac{C(t)}{C_0} \right] = -\lambda t \quad (4)$$

In this study, the pseudo-first-order model (Eq. (3)) was used to analyze the various MS2 inactivation experimental data sets collected. Also, the unknown inactivation parameter values  $\lambda_0$  and  $\alpha$  were obtained by fitting Eq. (3) to the experimental log-normalized-concentration data using non-linear least squares algorithms, whereas the unknown parameter  $\lambda$  was estimated by linear regression fit of Eq. (4) to the log-normalized experimental data.

### 4. Results and discussion

#### 4.1. MS2 inactivation in the absence of quartz sand

Fig. 3 shows the experimental data from the batch experiments of MS2 inactivation by TiO<sub>2</sub> NPs under light and dark conditions at 25 °C without the presence of quartz sand for the three different initial virus concentrations. The fitted MS2 inactivation parameter

values ( $\lambda_0$ ,  $\alpha$ , and  $\lambda$ ) for ambient light and dark conditions in both controls and reactors are listed in Table 1. It should be noted that normalized MS2 concentrations over 1 are due to slight variations in the initial concentration of the virus suspensions present in each tube. The experimental data were fitted with both the time-dependent inactivation model and the time-invariant inactivation model. The parameters  $\lambda_0$  and  $\alpha$  were determined by fitting Eq. (3) to the observed normalized MS2 log-concentrations, whereas  $\lambda$  values were determined by linear regression fit to Eq. (4) of the same experimental data. The fitted MS2 inactivation parameter values ( $\lambda_0$ ,  $\alpha$ , and  $\lambda$ ) are listed in Table 1. Note that only simulated concentrations based on the time-dependent inactivation are shown in Fig. 3 because the time-dependent inactivation model matched the experimental inactivation data much better than the constant inactivation model.

The experimental results showed that in the absence of sand with ambient light, the virus inactivation rates were higher compared to the virus inactivation rates under dark conditions, except for the cases of higher virus concentrations where the opposite was observed (Table 1). Note that, in most cases similar inactivation rates were observed in reactor and control tubes (absence of TiO<sub>2</sub> NPs), suggesting that low TiO<sub>2</sub> concentrations affect only slightly MS2 inactivation with and without ambient light. However, TiO<sub>2</sub> photocatalytic oxidation under UV irradiation may be a viable option for inactivating viruses in drinking water [59]. Gerrity et al. [59] tested different bacteriophages (MS2, PRD1,  $\Phi$ X174, and fr) that showed different inactivation behaviors, suggesting the lack of knowledge of how virus structure leads to differences

in photocatalytic inactivation kinetics. Previous studies showed that virus inactivation rates decrease with increasing initial virus concentration [56,60]. However, in this study, no clear trend was observed.

#### 4.2. MS2 inactivation in the presence of quartz sand

Fig. 4 shows the experimental data from the batch experiments of MS2 inactivation by TiO<sub>2</sub> NPs under light and dark conditions at 25 °C with the presence of quartz sand, for the three different initial virus concentrations. The fitted MS2 inactivation parameter values ( $\lambda_0$ ,  $\alpha$ , and  $\lambda$ ), for the experiments in the presence of quartz sand with and without ambient light, in the control and reactor tubes, are listed in Table 1. The presence of quartz sand affects virus inactivation by TiO<sub>2</sub> NPs under both ambient light and dark conditions, with generally faster inactivation without the presence of quartz sand (see Table 1). It was observed that, under the present experimental conditions, the attachment of viruses onto quartz sand offers a protection against inactivation, which is in agreement with previous studies [56]. However, attachment has been shown to produce a range of outcomes, from increasing inactivation, to having no effect, to protecting viruses from inactivation [3]. Note that the double agar overlay method, which is used for MS2 enumeration, measures the capacity of MS2 to infect, and provides incomplete information about the attached viruses. Moreover, TiO<sub>2</sub> NPs significantly attach onto sand surfaces, with the surface charge being a primary factor in their attachment [43,61,62]. Note that, the extent of nanoparticle adhesion onto sil-

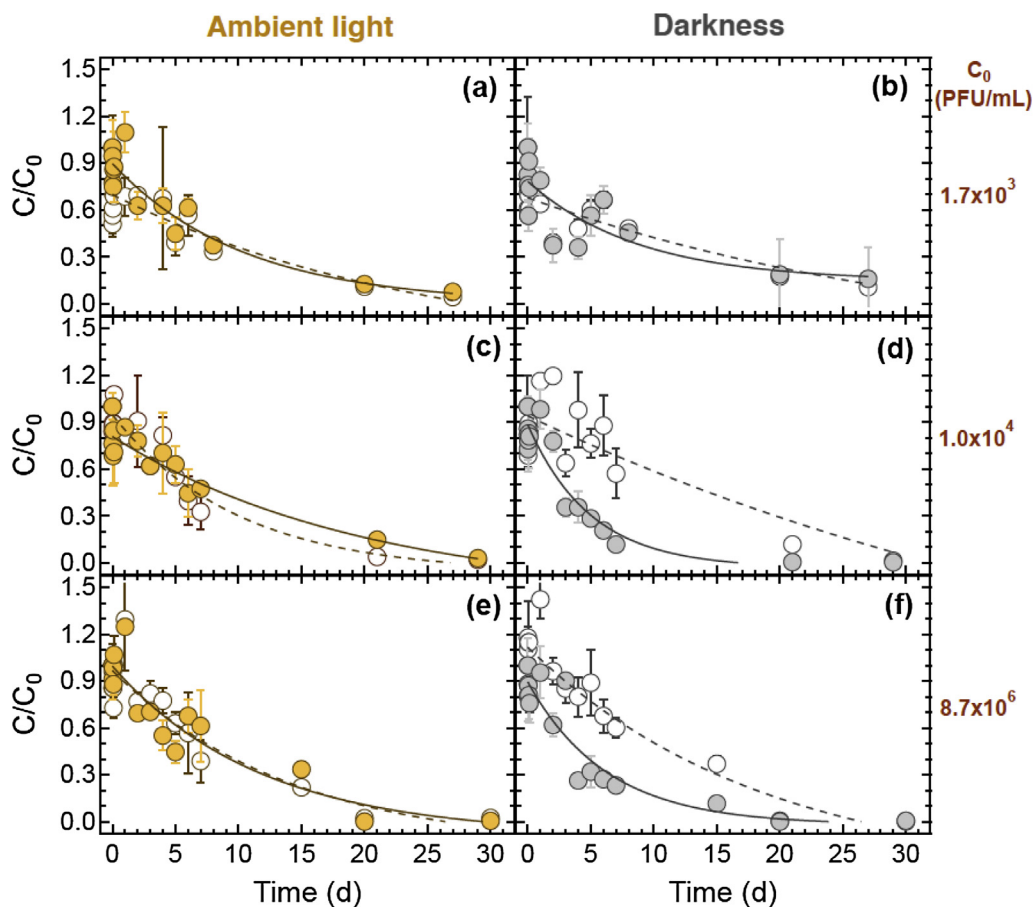


**Fig. 3.** Experimental data of MS2 inactivation by TiO<sub>2</sub> NPs with and without ambient light in reactor (solid symbols) and control (open symbols) tubes for initial concentration: (a, b)  $C_0 = 1.7 \pm 0.22 \times 10^3$ , (c, d)  $C_0 = 1 \pm 0.14 \times 10^4$ , and (e, f)  $C_0 = 8.7 \pm 1.8 \times 10^6$  PFU/mL. The solid and dashed curves correspond to the simulated normalized concentration histories for experiments conducted in reactor and control tubes, respectively. Error bars not shown are smaller than the size of the symbol.  $R^2$  values: 0.79–0.98.

**Table 1**  
Fitted MS2 inactivation parameters.

Experimental conditions	Initial virus concentration $C_0$ (PFU/mL)	Controls				Reactors			
		$\lambda_0$ (day <sup>-1</sup> )	$\alpha$ (day <sup>-1</sup> )	$\lambda$ (day <sup>-1</sup> )	$R^2$	$\lambda_0$ (day <sup>-1</sup> )	$\alpha$ (day <sup>-1</sup> )	$\lambda$ (day <sup>-1</sup> )	$R^2$
<i>Ambient light</i>									
ddH <sub>2</sub> O	$2.1 \pm 0.59 \times 10^4$	0.49	0.024	0.298	0.98	0.384	0.003	0.394	0.91
PBS	$1.7 \pm 0.22 \times 10^3$	0.188	0.038	0.117	0.93	0.156	0.033	0.101	0.96
PBS	$1 \pm 0.14 \times 10^4$	0.201	0.037	0.144	0.98	0.136	0.032	0.112	0.95
PBS	$8.7 \pm 1.8 \times 10^6$	0.098	0.032	0.136	0.91	0.247	0.165	0.115	0.87
<i>Darkness</i>									
ddH <sub>2</sub> O	$2.1 \pm 0.59 \times 10^4$	0.219	0.014	0.154	0.96	0.112	0.019	0.129	0.97
PBS	$1.7 \pm 0.22 \times 10^3$	0.248	0.084	0.088	0.87	0.237	0.085	0.079	0.79
PBS	$1 \pm 0.14 \times 10^4$	0.037	0.006	0.126	0.89	0.385	0.073	0.239	0.98
PBS	$8.7 \pm 1.8 \times 10^6$	0.065	0.008	0.21	0.92	0.212	0.033	0.172	0.89
<i>Ambient light + sand</i>									
ddH <sub>2</sub> O	$2.1 \pm 0.59 \times 10^4$	0.209	0.007	0.248	0.99	0.948	0.03	0.43	0.98
PBS	$1.7 \pm 0.22 \times 10^3$	0.124	0.019	0.099	0.96	0.193	0.039	0.122	0.95
PBS	$1 \pm 0.14 \times 10^4$	0.397	0.07	0.115	0.90	0.072	0.018	0.051	0.84
PBS	$8.7 \pm 1.8 \times 10^6$	0.236	0.156	0.068	0.88	0.234	0.149	0.059	0.86
<i>Darkness + sand</i>									
ddH <sub>2</sub> O	$2.1 \pm 0.59 \times 10^4$	0.274	0.011	0.229	0.99	0.401	0.005	0.36	0.88
PBS	$1.7 \pm 0.22 \times 10^3$	0.28	0.054	0.139	0.94	0.318	0.11	0.078	0.81
PBS	$1 \pm 0.14 \times 10^4$	0.125	0.024	0.079	0.89	0.119	0.032	0.078	0.88
PBS	$8.7 \pm 1.8 \times 10^6$	0.097	0.268	0.109	0.90	1.194	0.314	0.069	0.88

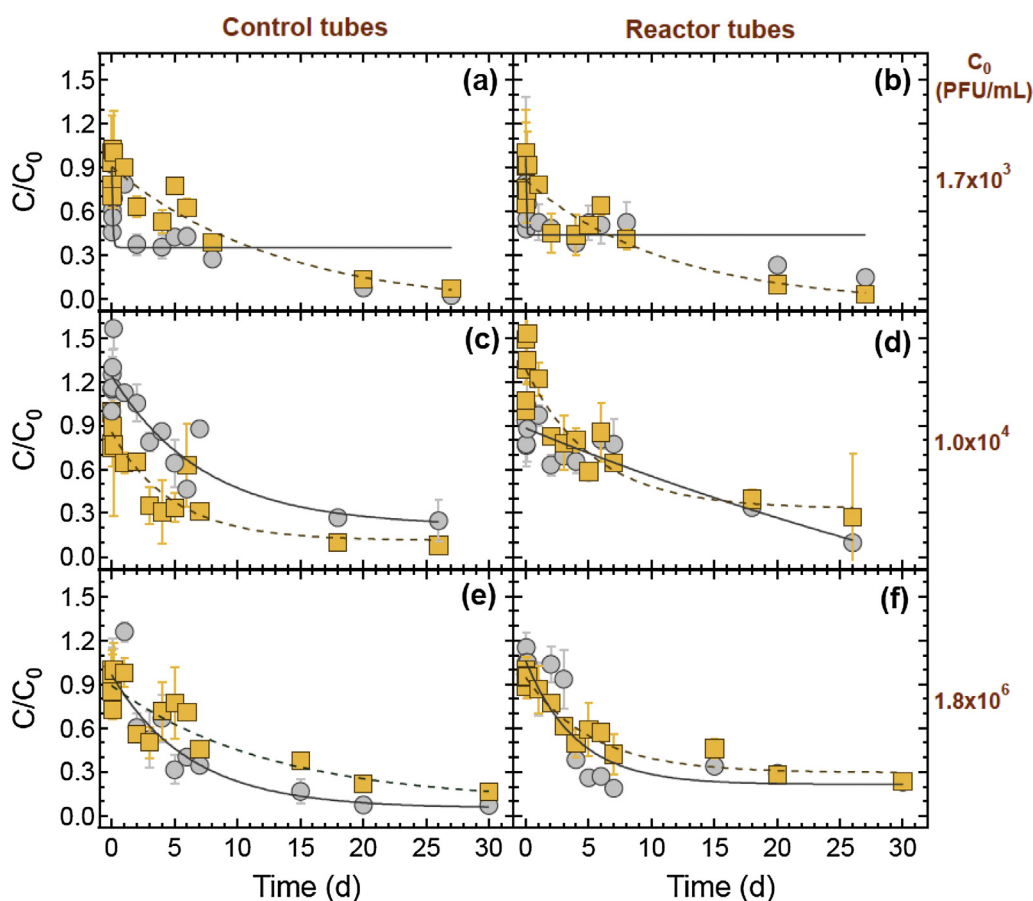


**Fig. 4.** Experimental data of MS2 inactivation by TiO<sub>2</sub> NPs in reactor and control tubes, in the presence of quartz sand with ambient light (squares) and darkness (circles), for initial concentration: (a, b)  $C_0 = 1.7 \pm 0.22 \times 10^3$ , (c, d)  $C_0 = 1 \pm 0.14 \times 10^4$ , and (e, f)  $C_0 = 8.7 \pm 1.8 \times 10^6$  PFU/mL. The solid and dashed curves correspond to the simulated concentration histories for experiments conducted in the darkness and in the presence of ambient light, respectively. Error bars not shown are smaller than the size of the symbol.  $R^2$  values: 0.81–0.99.

ica grains increases with increasing nanoparticle concentration [63]. Furthermore, TiO<sub>2</sub> NPs immobilised onto quartz sand (SiO<sub>2</sub>) exhibit enhanced photoactivity, caused by the diffusion of Si atoms from the underlying sand into the TiO<sub>2</sub> coating [64].

Fig. 5 shows that TiO<sub>2</sub> NPs can inactivate MS2 viruses in water under both ambient light and dark conditions, and that, with the only exception of the lower initial virus concentration, the presence of quartz sand hinders virus inactivation. Moreover, in the

presence of sand, low initial virus concentrations yielded higher inactivation rates  $\lambda$ , compared to high initial virus concentrations, while in the absence of sand no clear trend was observed. However, MS2 inactivation results varied substantially among the replicates, suggesting formation of viral aggregates in presence of Ti metal ions, as noted and by other investigators [65,66].

The photosensitive TiO<sub>2</sub> NPs were found to be harmful for MS2 to varying degrees under ambient light and dark conditions. The presence of light irradiation has been found to be a significant factor, presumably due to its role in promoting generation of reactive oxygen species (ROS) such as hydroxyl (OH<sup>•</sup>) and superoxide anion (O<sub>2</sub><sup>•-</sup>) radicals. It should be noted however that, virus inactivation under UV irradiated TiO<sub>2</sub> can be attributed mainly to the damages of capsid proteins inflicted by OH<sup>•</sup> and O<sub>2</sub><sup>•-</sup> followed by the viral nucleic acid fragmentation [47,67,68]. Moreover, higher resistance of viruses than bacteria to photocatalytic processes has been observed [69,70]. Also, non-enveloped viruses were found to be more prone to the oxidizing activity of OH<sup>•</sup> radicals than enveloped viruses [27,28]. Koizumi and Taya [26] observed significant MS2 inactivation by TiO<sub>2</sub> only with light irradiation. Furthermore, Lee and Ko [71] showed remarkable rates of MS2 inactivation by UV-A and UV-B in the presence of TiO<sub>2</sub> NPs. Also, Li et al. [72] observed that the rate of the MS2 virus removal was comparable with and without visible light illumination. During photocatalytic oxidation of MS2, the virus may be inactivated by damaging the A protein and preventing interaction with host cells or inhibiting lifecycle processes after the A protein enters the host. Damage to the coat proteins of MS2 can expose the RNA to damaging ROS or change the capsid conformation and preventing the A protein from interacting with bacterial pili [28,73,74]. However, in this study MS2 inactivation was also observed under ambient light and dark conditions in both absence and presence of quartz sand, indicating that undetermined mechanisms in addition to photocatalytic ROS production were responsible for virus inactivation.

#### 4.3. MS2 inactivation in ddH<sub>2</sub>O and PBS

Fig. 6 shows a comparison between MS2 inactivation data in ddH<sub>2</sub>O and PBS in the presence and absence of quartz sand with and without ambient light. Note that similar initial virus concentration ( $C_0 \sim 10^4$  PFU/mL) was used in both ddH<sub>2</sub>O and PBS sets of experiments. The fitted MS2 inactivation parameter values ( $\lambda_0$ ,  $\alpha$  and  $\lambda$ ) are listed in Table 1. In most cases, in the presence and absence of quartz sand, higher MS2 inactivation rates were observed in ddH<sub>2</sub>O than in PBS solution for both control tubes (Fig. 6a, c, e, g) and reactor tubes (Fig. 6b, d, f, h). This is attributed to possible increased MS2 aggregation in PBS solution due to binding of phosphate to positively charged lysine, a hydrophilic amino acid residue found at MS2 proteins [7,75]. Virus aggregation is known to significantly reduce inactivation. Worthy to note is that, viral aggregation in PBS has been observed in many studies and is known to influence electrokinetic measurements [7,75,76]. Moreover, virus surface proteins could be adsorbed onto TiO<sub>2</sub> NP surfaces through electrostatic, hydrophobic or specific chemical interactions, with phosphate ions playing an important role in the attachment/detachment process and the TiO<sub>2</sub> NP stability [77]. Furthermore, higher virus inactivation rates were observed in reactors than controls under both ambient light and dark conditions in ddH<sub>2</sub>O, while in PBS no clear trend was observed. Note that in a similar study, murine norovirus inactivation in PBS by 10 mg/L P25 TiO<sub>2</sub> was altered only slightly with UV254 irradiation [78]. Thus, PBS in comparison to ddH<sub>2</sub>O was found to inhibit TiO<sub>2</sub>, making PBS a poor choice for MS2 inactivation. The experimental results of this work indicate that ambient light plays a significant role in virus inactivation in ddH<sub>2</sub>O, especially in the absence of quartz sand (see Fig. 6d).

MS2 removal in batch experiments primarily relies on virus interactions with the surrounding environment (TiO<sub>2</sub> NPs and quartz sand) through attachment, charge neutralization [79],

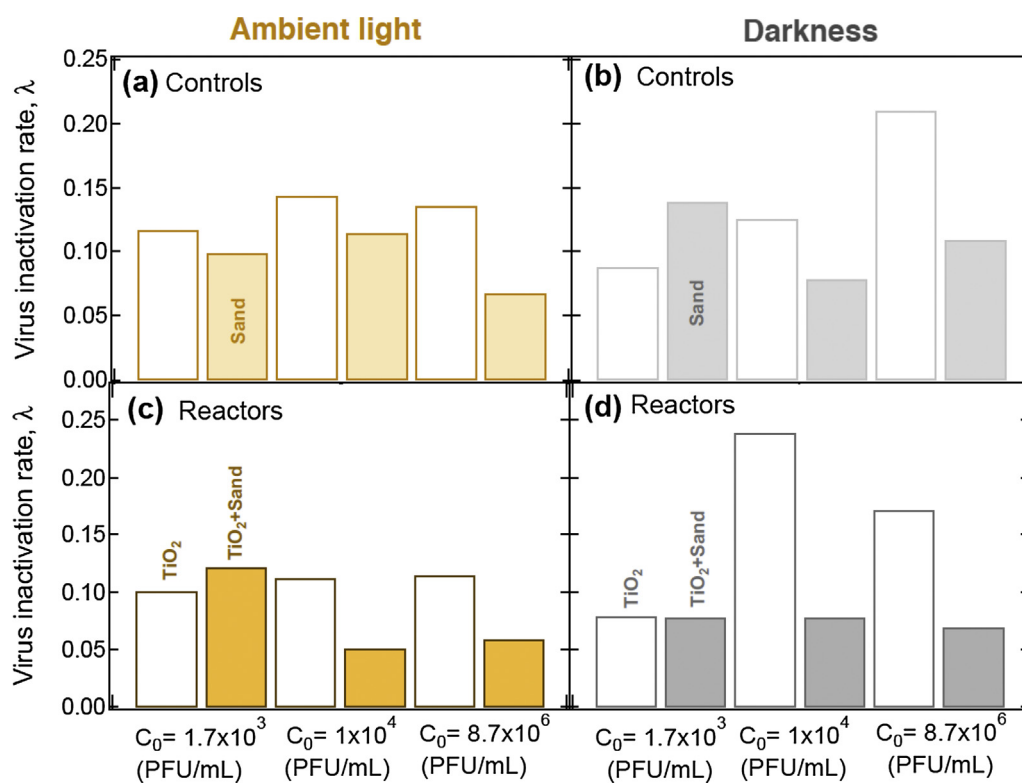
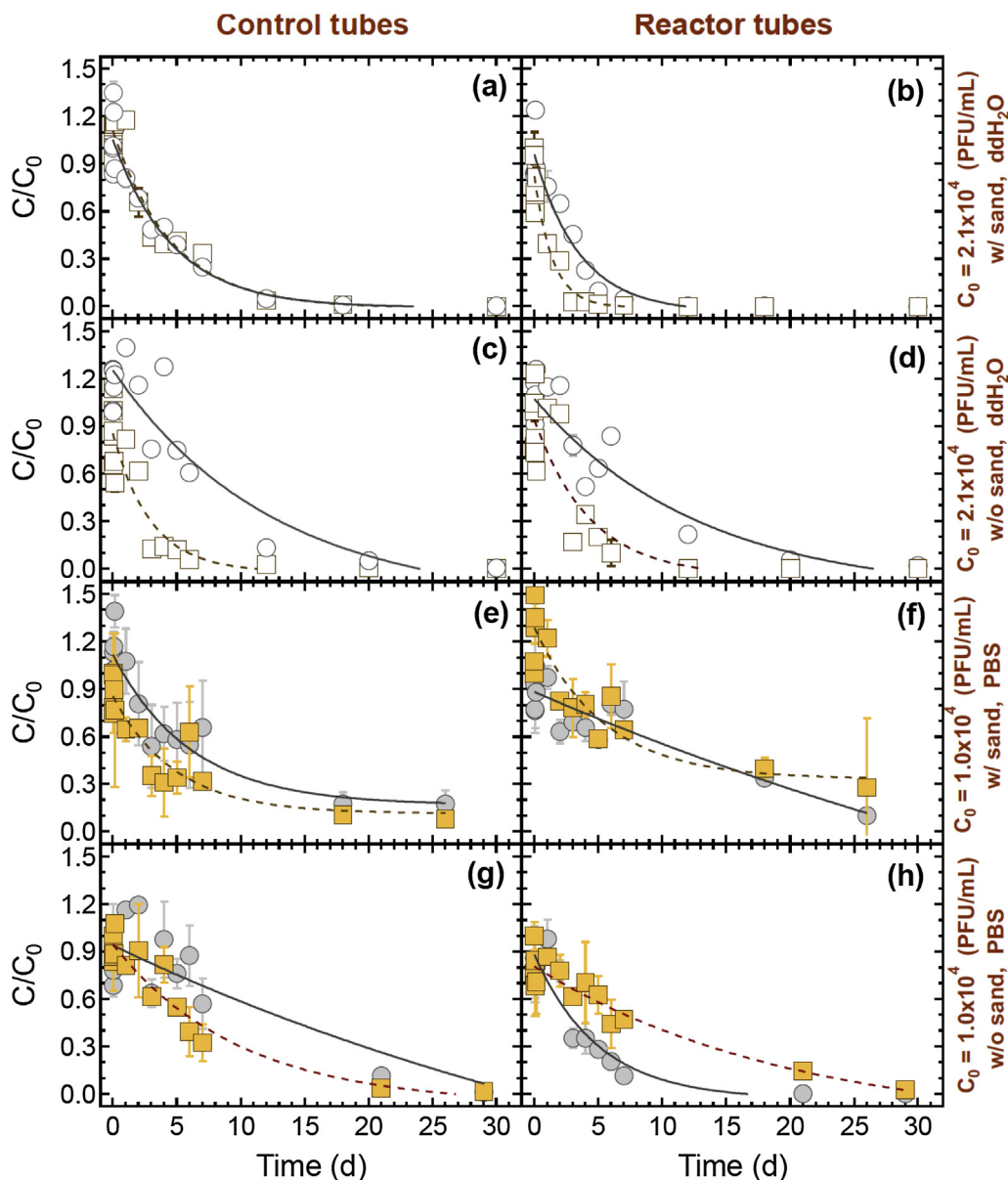


Fig. 5. Estimated inactivation rate,  $\lambda$ , for several initial virus concentrations: (a, c) with and (b, d) without ambient light, in (a, b) controls and (c, d) reactors.



**Fig. 6.** Comparison between MS2 batch inactivation experimental data in ddH<sub>2</sub>O (open symbols) and PBS (solid symbols), in reactor and control tubes, with ambient light (squares) and darkness (circles), for initial concentration: (a–d)  $C_0 = 2.1 \pm 0.59 \times 10^4$ , and (e–h)  $C_0 = 1 \pm 0.14 \times 10^4$  PFU/mL. The solid and dashed curves correspond to the simulated normalized concentration histories for experiments conducted in the darkness and in the presence of ambient light, respectively. Error bars not shown are smaller than the size of the symbol.  $R^2$  values: 0.84–0.99.

and hydrophobic interactions [80]. Thus, an MS2 suspension destabilizes resulting in virus aggregation and separation via gravity sedimentation or attachment onto TiO<sub>2</sub> NPs and quartz sand. Quartz sand provides virus protection against the disruption of the coat protein and degradation of the nucleic acid [81]. Moreover, virus attachment is generally assumed to be controlled by virus characteristics such size, shape, and isoelectric point and surface charge [82]. Electrostatic repulsion occurs between MS2 and TiO<sub>2</sub> NPs, because the surfaces of TiO<sub>2</sub> NPs under the experimental conditions (PBS, pH = 7,  $I_s = 2$  mM) are negatively charged, and MS2 surfaces have both hydrophobic and negatively charged hydrophilic regions [47,83]. Therefore, MS2 attachment onto TiO<sub>2</sub> NPs is unfavorable, and MS2 inactivation is hypothesized to be mediated by the bulk phase free TiO<sub>2</sub> NPs, not by the MS2 surface-bound TiO<sub>2</sub> NPs [22]. However, it is worthy to note that MS2 particles are multilayered soft (or permeable) particles with the inner RNA and the outer proteic capsid. Both of these components are permeable to external fluid flow and the

density of their charges is neutralized at pH values equal to 2.9 and 9, respectively [76]. Thus, in theory the proteic capsid of MS2 carries at a pH of 7 a positive net charge, while the inner RNA is negatively charged under such a pH condition [84]. However, the stability of MS2 suspension may not follow the classical DLVO theory. Duval et al. [85] suggested that the sign and magnitude of the electrostatic interactions between multilayered particles depend on the charges of the layers located within a depth on the order of the Debye length.

## 5. Conclusions

Previous works by our group demonstrated that the presence of quartz sand is effective at inactivating MS2 [6,56]. Our previous results, in conjunction with the inactivation of TiO<sub>2</sub>-attached contaminants, led us to investigate if the combination of TiO<sub>2</sub>, quartz sand and ambient light could also promote MS2 inactivation. To test this hypothesis, batch experiments were performed in order

to examine the ability of TiO<sub>2</sub> NPs to inactivate MS2 viruses at low exposure conditions (10 mg/L) in the presence of quartz sand with and without ambient light, representing conditions of surface and subsurface aquatic environments, respectively. The photoinactivation of MS2 by TiO<sub>2</sub> NPs in the presence of quartz sand was measured by assaying total MS2 infectivity, both attached and suspended, in the presence of ambient light and in the dark. In most cases, the presence of quartz sand hinders MS2 inactivation by TiO<sub>2</sub> NPs under both ambient light and dark conditions. Therefore, it is hypothesized that MS2 is protected by attachment onto quartz sand. Most probably, the attached TiO<sub>2</sub> NPs onto quartz sand block the migration of electrons to TiO<sub>2</sub> NPs and hence reduce possible ROS production, which in turn decreases MS2 inactivation. In contrast, diffusion of Si from the quartz sand into the TiO<sub>2</sub> lattice was found to enhance TiO<sub>2</sub> photoactivity [64,86]. Most MS2 samples in ambient light showed an increase in inactivation, with higher inactivation occurring in ddH<sub>2</sub>O than PBS buffer conditions. MS2 in the presence of quartz sand showed lower levels of inactivation by TiO<sub>2</sub> NPs in ambient light exposure. Similar inactivation of total MS2 occurred in the dark, suggesting that the key factors controlling MS2 inactivation by TiO<sub>2</sub> NPs were: (1) attachment onto quartz sand, and (2) exposure to ambient light.

Given that TiO<sub>2</sub> is one of the most utilized nanomaterials in consumer products, TiO<sub>2</sub> NPs eventually enter the water supplies or wastewater treatment plants. Consequently, TiO<sub>2</sub> NP interaction with aquatic pathogenic viruses is of primary consideration. Even when associated with TiO<sub>2</sub> NPs, viruses tend to remain in suspension and pass through granular media filters. Actually, it is anticipated that TiO<sub>2</sub> NPs will serve as carriers for pathogenic microorganisms. In conjunction with exposure to ambient light, TiO<sub>2</sub> NPs can be expected to inactivate viruses with morphological structures similar to that of MS2. However, further research is needed in order to enhance TiO<sub>2</sub> based virus inactivation, which is a relatively slow process, to thoroughly understand the molecular mechanisms by which viruses are inactivated and physically removed, and to investigate the associated consequences on ecosystems. Certainly, to improve the microbial quality of the water, and to identify novel approaches that control viruses in aquatic environments, it would be desirable to differentiate virus attachment and inactivation by evaluating these two processes separately.

## Acknowledgments

This research has been co-financed by the European Union (European Social Fund-ESF) and Greek national funds through the Operational program “Education and Lifelong Learning” of the National Strategic Reference Framework (NSRF)-Research Funding Program: Aristeia I (Code 1185).

## Appendix A. Supplementary material

Supplementary data associated with this article can be found, in the online version, at <http://dx.doi.org/10.1016/j.jcis.2017.02.059>.

## References

- [1] C. Masciopinto, R. La Mantia, C.V. Chrysikopoulos, Fate and transport of pathogens in a fractured aquifer in the Salento area, Italy, *Water Resour. Res.* 44 (2008) W01404, <http://dx.doi.org/10.1029/2006WR005643>.
- [2] C.V. Chrysikopoulos, C. Masciopinto, R. La Mantia, I.D. Manariotis, Removal of biocolloids suspended in reclaimed wastewater by injection in a fractured aquifer model, *Environ. Sci. Technol.* 44 (2010) 971–977.
- [3] S.B. Grant, E.J. List, M.E. Lidstrom, Kinetic analysis of virus adsorption and inactivation in batch experiments, *Water Resour. Res.* 29 (1993) 2067–2085.
- [4] J.P. Loveland, J.N. Ryan, G.L. Amy, R.W. Harvey, The reversibility of virus attachment to mineral surfaces, *Colloids Surf. A: Physicochem. Eng. Aspects* 107 (1996) 205–221.
- [5] Y. Chu, Y. Jin, M. Flury, M.V. Yates, Mechanisms of virus removal during transport in unsaturated porous media, *Water Resour. Res.* 37 (2001) 253–263.
- [6] R. Anders, C.V. Chrysikopoulos, Evaluation of the factors controlling the time dependent inactivation rate coefficient of bacteriophage MS2 and PRD1, *Environ. Sci. Technol.* 40 (2006) 3237–3242.
- [7] V.I. Syngouna, C.V. Chrysikopoulos, Interaction between viruses and clays in static and dynamic batch systems, *Environ. Sci. Technol.* 44 (12) (2010) 4539–4544, <http://dx.doi.org/10.1021/es100107a>.
- [8] V.I. Syngouna, C.V. Chrysikopoulos, Transport of biocolloids in water saturated columns packed with sand: effect of grain size and pore water velocity, *J. Contam. Hydrol.* 126 (2011) 301–314.
- [9] V.I. Syngouna, C.V. Chrysikopoulos, Cotransport of clay colloids and viruses in water saturated porous media, *Colloids Surf. A* 416 (2013) 56–65.
- [10] C.V. Chrysikopoulos, A.F. Aravantinou, Virus attachment onto quartz sand: role of grain size and temperature, *J. Environ. Chem. Eng.* 2 (2014) 796–801, <http://dx.doi.org/10.1016/j.jece.2014.01.025>.
- [11] M. Bellou, V.I. Syngouna, M.A. Tselepi, P.A. Kokkinos, S.C. Paparradopoulos, C.V. Chrysikopoulos, A. Vantarakis, Interaction of human adenovirus and coliphages with kaolinite and bentonite, *Sci. Total Environ.* 517 (2015) 86–95.
- [12] M.R. Wiesner, G.V. Lowry, P. Alvarez, D. Dionysiou, P. Biswas, Assessing the risks of manufactured nanomaterials, *Environ. Sci. Technol.* 40 (2006) 4336–4345.
- [13] N.C. Mueller, B. Nowack, Exposure modeling of engineered nanoparticles in the environment, *Environ. Sci. Technol.* 42 (2008) 4447–4453.
- [14] C.O. Robichaud, A.E. Uyar, M.R. Darby, L.G. Zucker, M.R. Wiesner, Estimates of upper bounds and trends in nano-TiO<sub>2</sub> production as a basis for exposure assessment, *Environ. Sci. Technol.* 43 (2009) 4227–4233, <http://dx.doi.org/10.1021/es8032549>.
- [15] I. Chowdhury, D.M. Cwiertny, S.L. Walker, Combined factors influencing the aggregation and deposition of nano-TiO<sub>2</sub> in the presence of humic acid and bacteria, *Environ. Sci. Technol.* 46 (2012) 6968–6976, <http://dx.doi.org/10.1021/es2034747>.
- [16] N. Nolan, S. Pillai, M. Seery, Spectroscopic investigation of the anatase-to rutile transformation of sol-gel-synthesized TiO<sub>2</sub> photocatalysts, *J. Phys. Chem. C* 113 (2009) 16151–16157.
- [17] M.A. Ferguson, M.R. Hoffmann, J.G. Hering, TiO<sub>2</sub>-photocatalyzed As(III) oxidation in aqueous suspensions: reaction kinetics and effects of adsorption, *Environ. Sci. Technol.* 39 (2005) 1880–1886.
- [18] M.A. Kiser, P. Westerhoff, T. Benn, Y. Wang, J. PePrez-Rivera, K. Hristovski, Titanium nanomaterial removal and release from wastewater treatment plants, *Environ. Sci. Technol.* 43 (17) (2009) 6757–6763.
- [19] N. O'Brien, E. Cummins, Ranking initial environmental and human health risk resulting from environmentally relevant nanomaterials, *J. Environ. Sci. Health, Part A: Toxic/Hazard. Subst. Environ. Eng.* 45 (2010) 992–1007.
- [20] T.M. Scown, R. van Aerle, C.R. Tylre, Review: do engineered nanoparticles pose a significant threat to the aquatic environment?, *Crit. Rev. Toxicol.* 40 (2010) 653–670.
- [21] R.J. Watts, S.H. Kong, M.P. Orr, G.C. Miller, B.E. Henry, Photocatalytic inactivation of coliform bacteria and viruses in secondary waste-water effluent, *Water Res.* 29 (1) (1995) 95–100.
- [22] M. Cho, H. Chung, J. Yoon, Different inactivation behaviors of MS2 phage and *Escherichia coli* in TiO<sub>2</sub> photocatalytic disinfection, *Appl. Environ. Microbiol.* 71 (1) (2005) 270–275.
- [23] K. Page, R.G. Palgrave, I.P. Parkin, M. Wilson, S.L.P. Savin, A.V. Chadwick, Titania and silver-titania composite films on glass-potent antimicrobial coatings, *J. Mater. Chem.* 17 (1) (2007) 95–104.
- [24] S. Dalai, S. Pakrashi, R.S. SureshKumar, N. Chandrasekaran, N. Mukherjee, A comparative cytotoxicity study of TiO<sub>2</sub> nanoparticles under light and dark conditions at low exposure concentrations, *Toxicol. Res.* 1 (2012) 116–130.
- [25] Y. Kikuchi, K. Sunada, T. Iyoda, K. Hashimoto, A. Fujishima, Photocatalytic bactericidal effect of TiO<sub>2</sub> thin films: dynamic view of the active oxygen species responsible for the effect, *J. Photochem. Photobiol. A: Chem.* 106 (1997) 51–56.
- [26] Y. Koizumi, M. Taya, Kinetic evaluation of biocidal activity of titanium dioxide against phage MS2 considering interaction between the phage and photocatalyst particles, *Biochem. Eng. J.* 12 (2) (2002) 107–116.
- [27] M.V. Liga, E.L. Bryant, V.L. Colvin, Q.L. Li, Virus inactivation by silver doped titanium dioxide nanoparticles for drinking water treatment, *Water Res.* 45 (2) (2011) 535–544.
- [28] M.V. Liga, S.J. Maguire-Boyle, H.R. Jafry, A.R. Barron, Q. Li, Silica decorated TiO<sub>2</sub> for virus inactivation in drinking water—simple synthesis method and mechanisms of enhanced inactivation kinetics, *Environ. Sci. Technol.* 47 (12) (2013) 6463–6470.
- [29] M. Otaki, T. Hirada, S. Ohgaki, Aqueous microorganisms inactivation by photocatalytic reaction, *Water Sci. Technol.* 42 (2000) 103–108.
- [30] J. Marugan, R. van Grieken, C. Pablos, C. Sordo, Analogies and differences between photocatalytic oxidation of chemicals and photocatalytic inactivation of microorganisms, *Water Res.* 44 (3) (2006) 789–796.
- [31] H.A. Foster, I.B. Ditta, S. Varghese, A. Steele, Photocatalytic disinfection using titanium dioxide: spectrum and mechanism of antimicrobial activity, *Appl. Microbiol. Biotechnol.* 90 (2011) 1847–1868.
- [32] M.A. Butkus, M.P. Labare, J.A. Starke, K. Moon, M. Talbot, Use of aqueous silver to enhance inactivation of coliphage MS2 by UV disinfection, *Appl. Environ. Microbiol.* 70 (5) (2004) 2848–2853.
- [33] R.V. Rai, J.A. Bai, Nanoparticles and their potential application as antimicrobials, A. Méndez-Vilas (Ed.), *Science Against Microbial Pathogens*,

- Communicating Current Research and Technological Advances, 2011, pp. 197–209.
- [34] D. Zhao, X. Yang, C. Chen, X. Wang, Enhanced photocatalytic degradation of methylene blue on multiwalled carbon nanotubes–TiO<sub>2</sub>, *J. Colloid Interf. Sci.* 398 (2013) 234–239.
- [35] A. Nel, T. Xia, L. Mädler, N. Li, Toxic potential of materials at the nanolevel, *Science* 311 (2006) 622–627.
- [36] T.C. Long, N. Saleh, R.D. Tilton, G.V. Lowry, B. Veronesi, Titanium dioxide (P25) produces reactive oxygen species in immortalized brain microglia (BV2): implications for nanoparticle neurotoxicity, *Environ. Sci. Technol.* 40 (14) (2006) 4346–4352.
- [37] T. Xia, M. Kovochich, M. Liong, L. Madler, H. Shi, J.I. Yeh, J.I. Zink, A.E. Nel, Comparison of the mechanism of toxicity of zinc oxide and cerium oxide nanoparticles based on dissolution and oxidative stress properties, *ACS Nano* 2 (2008) 2121–2134.
- [38] M. Pelaez, N.T. Nolan, S.C. Pillai, M.K. Seery, P. Falaras, A.G. Kontos, P.S.M. Dunlop, J.W.J. Hamilton, J.A. Byrne, K. O'shea, M.H. Entezari, D.D. Dionysiou, A review on the visible light active titanium dioxide photocatalysts for environmental applications, *Appl. Catal. B* 125 (2012) 331–349.
- [39] T.J. Battin, F.V.D. Kammer, A. Weilharter, S. Ottofuelling, T. Hofmann, Nanostructured TiO<sub>2</sub>: transport behavior and effects on aquatic microbial communities under environmental conditions, *Environ. Sci. Technol.* 43 (2009) 8098–8104.
- [40] I. Fenoglio, G. Greco, S. Livraghi, B. Fubini, Non-UV-induced radical reactions at the surface of TiO<sub>2</sub> nanoparticles that may trigger toxic responses, *Chem. A-Eur. J.* 15 (2009) 4614–4621.
- [41] L.V. Zhukova, J. Kiwi, V.V. Nikandrov, Nanoparticles of TiO<sub>2</sub> cause aggregation of *Escherichia coli* cells and suppress their division at pH 4.0–4.5 in the absence of UV irradiation, *Dokl. Chem.* 435 (2010) 279–282.
- [42] M.H. Adams, Bacteriophages, Interscience, New York, NY, 1959, pp. 450–454.
- [43] K.A. Dunphy Guzman, M.P. Finnegan, J.F. Banfield, Influence of surface potential on aggregation and transport of titania nanoparticles, *Environ. Sci. Technol.* 40 (24) (2006) 7688–7693.
- [44] G. Chen, X. Liu, C. Su, Transport and retention of TiO<sub>2</sub> rutile nanoparticles in saturated porous media under low-ionic-strength conditions: measurements and mechanisms, *Langmuir* 27 (2011) 5393–5402.
- [45] B.J.R. Thio, D. Zhou, A.A. Keller, Influence of natural organic matter on the aggregation and deposition of titaniumdioxide nanoparticles, *J. Hazard. Mater.* 189 (1–2) (2011) 556–563.
- [46] M.B. Romanello, M.M. Fidalgo de Cortalezzi, An experimental study on the aggregation of TiO<sub>2</sub> nanoparticles under environmentally relevant conditions, *Water Res.* 47 (12) (2013) 3887–3898.
- [47] J.C. Sjogren, R.A. Sierka, Inactivation of phage MS2 by iron-aided titanium dioxide photocatalysis, *Appl. Environ. Microbiol.* 60 (1) (1994) 344–347.
- [48] T. Sato, M. Taya, Enhancement of phage inactivation using photocatalytic titanium dioxide particles with different crystalline structures, *Biochem. Eng. J.* 28 (3) (2006) 303–308.
- [49] Y. Sim, C.V. Chrysikopoulos, Analytical models for virus adsorption and inactivation in unsaturated porous media, *Colloids Surf. A: Physicochem. Eng. Aspects* 155 (1999) 189–197.
- [50] Y. Sim, C.V. Chrysikopoulos, Virus transport in unsaturated porous media, *Water Resour. Res.* 36 (1) (2000) 173–179.
- [51] Y. Sim, C.V. Chrysikopoulos, One-dimensional virus transport in porous media with time dependent inactivation rate coefficients, *Water Resour. Res.* 32 (8) (1996) 2607–2611.
- [52] M. Flury, W.A. Jury, Solute transport with residence-time-dependent sink/source reaction coefficients, *Water Resour. Res.* 35 (6) (1999) 1933–1938.
- [53] C.V. Chrysikopoulos, E.T. Vogler, Estimation of time dependent virus inactivation rates by geostatistical and resampling techniques: application to virus transport in porous media, *Stoch. Environ. Res. Risk Assess.* 18 (2004) 67–78.
- [54] S.A. Bradford, E. Segal, Fate of indicator microorganisms under nutrient management plan conditions, *J. Environ. Qual.* 38 (2009) 1728–1738.
- [55] C.S.P. Ojha, R.Y. Surampalli, P.K. Sharma, N. Joshi, Breakthrough curves and simulation of virus transport through fractured porous media, *J. Environ. Eng. (ASCE)* 137 (8) (2011) 731–739.
- [56] C.V. Chrysikopoulos, A.F. Aravantinou, Virus inactivation in the presence of quartz sand under static and dynamic batch conditions at different temperatures, *J. Hazard. Mater.* 233–234 (2012) 148–157.
- [57] C.V. Chrysikopoulos, I.D. Manariotis, V.I. Syngouna, Virus inactivation by high frequency ultrasound in combination with visible light, *Colloids Surf., B* 107 (2013) 174–179, <http://dx.doi.org/10.1016/j.colsurfb.2013.01.038>.
- [58] J.-A. Park, C.-G. Lee, S.-B. Kim, Influence of As(V) on bacteriophage MS2 removal by hematite in aqueous solutions, *Desalination. Water Treatment* 56 (2015) 760–769.
- [59] D. Gerrity, H. Ryu, J. Crittenden, M. Abbaszadegan, Photocatalytic inactivation of viruses using titanium dioxide nanoparticles and low-pressure UV light, *J. Environ. Sci. Health Part A* 43 (11) (2008) 1261–1270.
- [60] M.J. Mattle, B. Crouzy, M. Brennecke, K.R. Wigginton, P. Perona, T. Kohn, Impact of virus aggregation on inactivation by peracetic acid and implications for disinfectants, *Environ. Sci. Technol.* 45 (2011) 7710–7717.
- [61] C.C. Choy, M. Wazne, X. Meng, Application of an empirical transport model to simulate retention of nanocrystalline titanium dioxide in sand columns, *Chemosphere* 71 (2008) 1794–1801.
- [62] I.G. Godinez, C.J.G. Darnault, Aggregation and transport of nano-TiO<sub>2</sub> in saturated porous media: effects of pH, surfactants and flow velocity, *Water Res.* 45 (2011) 839–851.
- [63] A.E. Bayat, R. Junin, S. Shamshirband, W.T. Chong, Transport and retention of engineered Al<sub>2</sub>O<sub>3</sub>, TiO<sub>2</sub>, and SiO<sub>2</sub> nanoparticles through various sedimentary rocks, *Sci. Rep.* 5 (2015) 14264, <http://dx.doi.org/10.1038/srep14264>.
- [64] H.R. Jafry, M.V. Liga, Q. Li, A.R. Barron, Simple route to enhanced photocatalytic activity of P 25 titanium dioxide nanoparticles by silica addition, *Environ. Sci. Technol.* 45 (4) (2011) 1563–1568.
- [65] F.X. Abad, R.M. Pintó, J.M. Diez, A. Bosch, Disinfection of human enteric viruses in water by copper and silver in combination with low-levels of chlorine, *Appl. Environ. Microbiol.* 60 (7) (1994) 2377–2383.
- [66] J.I. Nieto-Juarez, K. Pierzchla, A. Sienkiewicz, T. Kohn, Inactivation of MS2 coliphage in Fenton and Fenton-like systems: role of transition metals, hydrogen peroxide and sunlight, *Environ. Sci. Technol.* 44 (9) (2010) 3351–3356.
- [67] N. Kashige, Y. Kakita, Y. Nakashima, F. Miake, K. Watanabe, Mechanism of the photocatalytic inactivation of *Lactobacillus casei* phage PL-1 by titania thin film, *Curr. Microbiol.* 42 (3) (2001) 184–189.
- [68] J.Y. Kim, C. Lee, M. Cho, J. Yoon, Enhanced inactivation of *E. coli* and MS-2 phage by silver ions combined with UV-A and visible light irradiation, *Water Res.* 42 (1–2) (2008) 356–362.
- [69] S. Josset, J. Taranto, N. Keller, V. Keller, M.C. Lett, Photocatalytic treatment of bioaerosols: impact of the reactor design, *Environ. Sci. Technol.* 44 (7) (2010) 2605–2611.
- [70] Y. Zhao, A.J. Aarnink, H. Xin, Inactivation of airborne *Enterococcus faecalis* and infectious bursal disease virus using a pilot-scale ultraviolet photocatalytic oxidation scrubber, *J. Air Waste Manag. Assoc.* 64 (1) (2014) 38–46.
- [71] J. Lee, G. Ko, Norovirus and MS2 inactivation kinetics of UV-A and UV-B with and without TiO<sub>2</sub>, *Water Res.* 47 (2013) 5607–5613.
- [72] Q. Li, M.A. Page, B.J. Marinas, J.K. Shang, Treatment of coliphage MS2 with palladium-modified nitrogen-doped titanium oxide photocatalyst illuminated by visible light, *Environ. Sci. Technol.* 42 (2008) 6148–6153.
- [73] M. Cho, J. Lee, Y. Mackeyev, L.J. Wilson, P.J.J. Alvarez, J.B. Hughes, J.H. Kim, Visible light sensitized inactivation of MS-2 bacteriophage by a cationic amine-functionalized C60 derivative, *Environ. Sci. Technol.* 44 (17) (2010) 6685–6691.
- [74] K.R. Wigginton, L. Menin, J.P. Montoya, T. Kohn, Oxidation of virus proteins during UV254 and singlet oxygen mediated inactivation, *Environ. Sci. Technol.* 44 (14) (2010) 5437–5443.
- [75] B. Yuan, M. Pham, T.H. Nguyen, Deposition kinetics of bacteriophage MS2 on a silica surface coated with natural organic matter in a radial stagnation point flow cell, *Environ. Sci. Technol.* 42 (2008) 7628–7633.
- [76] J. Langlet, F. Gaboriaud, J.F.L. Duval, C. Gantzer, Aggregation and surface properties of F-specific RNA phages: implication for membrane filtration processes, *Water Res.* 42 (2008) 2769–2777.
- [77] M.H. Nia, M. Rezaei-Tavirani, A.R. Nikoofar, H. Masoumi, R. Nasr, H. Hasanizadeh, M. Jadidi, M. Shadnush, Stabilizing and dispersing methods of TiO<sub>2</sub> nanoparticles in biological studies, *J. Paramed. Sci.* 6 (2) (2015). ISSN 2008–4978.
- [78] J. Lee, K. Zoh, G. Ko, Inactivation and UV disinfection of murine norovirus with TiO<sub>2</sub> under various environmental conditions, *Appl. Environ. Microbiol.* 74 (7) (2008) 2111–2117.
- [79] B.K. Mayer, H. Ryu, M. Abbaszadegan, Treatability of USEPA contaminant candidate list viruses: removal of coxsackievirus and echovirus using enhanced coagulation, *Environ. Sci. Technol.* 42 (18) (2008) 6890–6896.
- [80] J.F. Schijven, S.M. Hassanizadeh, Removal of viruses by soil passage: overview of modeling, processes, and parameters, *Crit. Rev. Environ. Sci. Technol.* 30 (1) (2000) 49–127.
- [81] G. Bitton, C.P. Gerba, *Groundwater Pollution Microbiology*, Wiley, New York, NY, 1984.
- [82] I. Xagorarakis, G.W. Harrington, P. Assavasilavasukul, J.H. Standridge, Removal of emerging waterborne pathogens and pathogen indicators by pilot-scale conventional treatment, *J. Am. Water Works Assoc.* 96 (5) (2004) 102–113.
- [83] C.V. Chrysikopoulos, V.I. Syngouna, Attachment of bacteriophages MS2 and ΦX174 onto kaolinite and montmorillonite: extended-DLVO interactions, *Colloids Surf., B* 92 (2012) 74–83, <http://dx.doi.org/10.1016/j.colsurfb.2011.11.028>.
- [84] C. Dika, J.F.L. Duval, H.M. Ly-Chatain, C. Merlin, C. Gantzer, Impact of Internal RNA on aggregation and electrokinetics of viruses: comparison between MS2 phage and corresponding virus-like particles, *Appl. Environ. Microbiol.* 77 (2011) 4939–4948.
- [85] J.F.L. Duval, J. Merlin, P.A.L. Narayana, Electrostatic interactions between diffuse soft multi-layered (bio)particles: beyond Debye-Huckel approximation and Deryagin formulation, *Phys. Chem. Chem. Phys.* 13 (2011) 1037–1053.
- [86] D.A.H. Hanaor, C.C. Sorrell, Sand supported mixed-phase TiO<sub>2</sub> photocatalysts for water decontamination applications, *Adv. Eng. Mater.* 16 (2) (2014) 248–254.